Inorg. Chem. **2003**, *42*, 3898–3906

Interpretation of the Magnetic Structures of $Cu_2Te_2O_5X_2$ (X = Cl, Br) and $Ca_{3.1}Cu_{0.9}RuO_6$ on the Basis of Electronic Structure Considerations: Cases for Strong Super-Superexchange Interactions Involving Cu^{2+} Ions

M.-H. Whangbo,* H.-J. Koo, and D. Dai

Department of Chemistry, North Carolina State University, Raleigh, North Carolina 27695-8204

D. Jung

Institute of Natural Science and Department of Chemistry, Wonkwang University, Iksan, Jeonbuk, South Korea 570-749

Received September 11, 2002

For super-superexchange interactions between Cu^{2+} ions, a qualitative rule was formulated to assess their strengths based on the geometrical parameters of the exchange paths. Spin dimer analysis was carried out for $Cu_2Te_2O_5X_2$ (X = Cl, Br) and $Ca_{3.1}Cu_{0.9}RuO_6$ to evaluate the relative strengths of their superexchange and super-superexchange interactions. The strongest antiferromagnetic interactions in $Cu_2Te_2O_5X_2$ (X = Cl, Br) are given by the super-superexchange interactions involving the most linear Cu–X···X–Cu paths between tetrahedral clusters $Cu_4O_8X_4$ along the ($a \pm b$)-directions. The adjacent $CuRuO_6$ chains of $Ca_{3.1}Cu_{0.9}RuO_6$ are antiferromagnetically coupled through the most linear Cu–O···O–Cu paths along the direction perpendicular to the plane of the CuRu zigzag chain. The spin lattices of $Cu_2Te_2O_5X_2$ and $Ca_{3.1}Cu_{0.9}RuO_6$ deduced from our spin dimer analysis are consistent with the available magnetic data. The spin lattice of a magnetic solid should be determined on the basis of appropriate electronic structure considerations.

1. Introduction

Energy states of a magnetic solid are commonly described by a Heisenberg spin Hamiltonian, which allows one to expresses excitation energies of a magnetic solid in terms of spin exchange parameters *J*. Experimentally, low-energy excitations of a magnetic solid are probed by magnetic susceptibility, neutron inelastic scattering, or Raman scattering measurements. When results of these experiments are analyzed in terms of a spin Hamiltonian, the spin exchange parameters are determined as numerical fitting parameters needed to reproduce the experimental data. As shown by the studies of $(VO)_2P_2O_7$ [1−6] and $CuWO_4$,[7,8] such an analysis does not necessarily lead to a unique set of *J* values because the result depends on what spin exchange paths one includes in the spin Hamiltonian. For instance, the magnetic susceptibility of ambient-pressure $(VO)_2P_2O_7$ is well described by the spin-$^1/_2$ alternating antiferromagnetic chain model[1,2] and also by the spin ladder model.[3,4]

In a magnetic solid of transition metal ions M whose first coordinate spheres are made up of main group ligand atoms L, spin exchange interactions between adjacent metal ions may take place through M−L−M superexchange (SE) paths or M−L···L−M super-superexchange (SSE) paths.[9−11] In predicting relative strengths of SE interactions, one can employ Goodenough rules[12] on the basis of the ∠M−L−M

* Author to whom correspondence should be addressed. E-mail: mike_whangbo@ncsu.edu.

(1) Johnston, D. C.; Saito, T.; Azuma, M.; Takano, M.; Yamauchi, T.; Ueda, Y. *Phys. Rev. B* **2001**, *64*, 134403 and the references therein.
(2) Johnston, D. C.; Johnson, J. W.; Goshorn, D. P.; Jacobson, A. J. *Phys. Rev. B* **1987**, *35*, 219.
(3) Barnes, T.; Riera, J. *Phys. Rev. B* **1994**, *50*, 6817.
(4) Eccleston, R. S.; Barnes, T.; Brody, J.; Johnson, J. W. *Phys. Rev. Lett*. **1994**, *73*, 2626.
(5) Garret, A. W.; Nagler, S. E.; Tennant, D. A.; Sales, B. C.; Barnes, T. *Phys. Rev. Lett*. **1997**, *79*, 745.
(6) Kikuchi, J.; Motoya, K.; Yamauchi, T.; Ueda, Y. *Phys. Rev. B* **1999**, *60*, 6731.
(7) Lake, B.; Tennant, D. A.; Cowley, R. A.; Axe, J. D.; Chen, C. K. *J. Phys.: Condens. Matter* **1996**, *8*, 8613.
(8) Ehrenberg, H.; Wiesmann, M.; Garcia-Jaca, J.; Weitzel, H.; Fuess, H. *J. Magn. Magn. Mater*. **1998**, *182*, 152.
(9) Koo, H.-J.; Whangbo, M.-H. *Inorg. Chem*. **2000**, *39*, 3599.
(10) Koo, H.-J.; Whangbo, M.-H.; VerNooy, P. D.; Torardi, C. C.; Marshall, W. J. *Inorg. Chem*. **2002**, *41*, 4664.
(11) Koo, H.-J.; Whangbo, M.-H. *Inorg. Chem*. **2001**, *40*, 2169.

10.1021/ic020551l CCC: $25.00
Published on Web 05/15/2003

angle, the symmetry properties of the metal d orbitals containing unpaired spins, and the number of unpaired spins at the metal site M. There have been no such qualitative rules for predicting the relative magnitudes of SSE interactions. As a result, in assigning strongly interacting spin exchange paths of a magnetic solid, one often neglects SSE interactions and is guided by intuition and the nature of the eigenvalue problem the supposed spin lattice generates. Consequently, as exemplified by the spin ladder model[3,4] for $(VO)_2P_2O_7$, the magnetic properties of a magnetic system can be explained in terms of a spin lattice that is quite irrelevant for the system. To avoid such an undesirable situation, it is important to assign spin lattices of magnetic solids on the basis of appropriate electronic structure considerations. The importance of the latter cannot be overemphasized in view of the fact that a SSE interaction can be stronger than any SE interaction in a given magnetic solid.[10,11]

In the present work we probe the question of assessing strongly interacting spin exchange paths of magnetic solids containing Cu^{2+} ions on both qualitative and semiquantitative levels. The qualitative approach is aimed at providing a tool for predicting whether SSE interactions are strong or weak by inspecting the geometrical parameters of their Cu−L···L−Cu paths, and the semiquantitative approach at estimating the relative strengths of SE and SSE interactions on an equal footing. As specific examples of magnetic solids containing Cu^{2+} ions, we examine the spin exchange interactions of $Cu_2Te_2O_5X_2$ (X = Cl, Br)[13−15] and $Ca_{3.1}Cu_{0.9}RuO_6$,[16] whose spin lattices were assigned without any electronic structure considerations. In section 2 we examine how the strength of a SSE interaction involving Cu^{2+} ions depends on the geometrical parameters of the Cu−L···L−Cu path to formulate a qualitative rule for assessing the strength of a SSE interaction. In section 3 we analyze the geometrical parameters associated with the SE and SSE interactions of $Cu_2Te_2O_5X_2$ and $Ca_{3.1}Cu_{0.9}RuO_6$ and show that the SSE interactions involving the most linear Cu−L···L−Cu paths, neglected in the earlier analyses, should be important according to the qualitative rule for SSE interactions. In section 4 we briefly discuss the method of spin dimer analysis to be used for our calculations.[9−11,17−21] Results of our spin dimer analysis for $Cu_2Te_2O_5X_2$ and $Ca_{3.1}Cu_{0.9}RuO_6$ are discussed in section 5. Finally, the essential findings of our work are summarized in section 6.

2. Qualitative Rule for Super-Superexchange Interactions between Cu^{2+} Ions

In general, a spin exchange parameter J is written as $J = J_F + J_{AF}$,[22,23] where the ferromagnetic term J_F (>0) is small so that the spin exchange becomes ferromagnetic (i.e., $J >$ 0) when the antiferromagnetic term J_{AF} (<0) is negligibly small in magnitude. Thus antiferromagnetic spin exchange interactions (i.e., $J < 0$) can be discussed by focusing on the J_{AF} terms.[9−11,17−21] The J_{AF} term for a SSE interaction varies as $J_{AF} \propto -S^2$, where S is the overlap integral between the two magnetic orbitals representing the two spin sites of a spin dimer (i.e., structural units containing two spin sites).

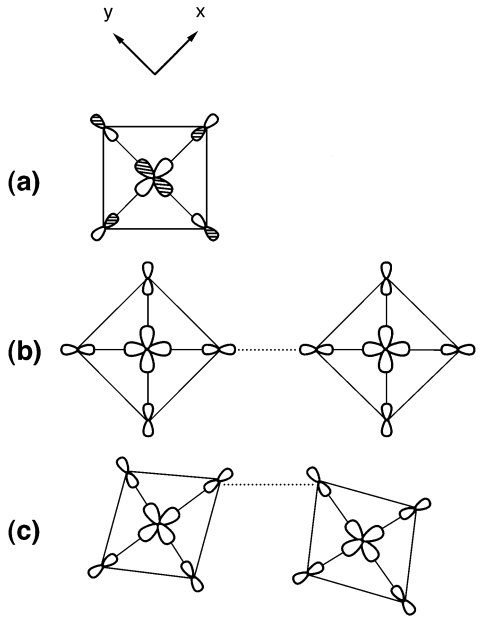

Figure 1. (a) Magnetic orbital of a square planar CuL_4 unit containing a Cu^{2+} ion. (b) Arrangement of two magnetic orbitals in a SSE interaction having a linear Cu−L···L−Cu path. (c) Arrangement of two magnetic orbitals in a SSE interaction having a nonlinear Cu−L···L−Cu path.

The strength of a SSE interaction depends critically on the overlap between the "p-orbital tails" of the two magnetic orbital tails associated with the M−L···L−M path.[9−11] The magnetic orbital of a square planar CuL_4 unit containing a Cu^{2+} ion is given by the $x^2 - y^2$ orbital of Cu, which makes σ antibonding interactions with the p orbitals of the four ligands L (Figure 1a). The overlap between two such magnetic orbitals associated with a SSE path Cu−L···L−Cu and, hence, the strength of the SSE interaction depend largely on the overlap between the two p orbitals residing on the main group atoms L of the L···L contact. Therefore, a qualitative rule for assessing the strength of a SSE interaction can be stated as follows: *the strength of the SSE interaction involving a path Cu−L···L−Cu should increase*

(12) Goodenough, J. B. *Magnetism and the Chemical Bond*; Wiley: Cambridge, MA, 1963.
(13) Johnsson, M.; Törnroos, K. W.; Mila, F.; Millet, P. *Chem. Mater*. **2000**, *12*, 2853.
(14) Lemmens, P.; Choi, K.-Y.; Güntherodt, G.; Johnsson, M.; Millet, P.; Mila, F.; Valenti, R.; Gros, C.; Brenig, W. *J. Phys. Chem. Solids* **2002**, *63*, 1115.
(15) Hay, P. J.; Thibeault, J. C.; Hoffmann, R. *J. Am. Chem. Soc*. **1975**, *97*, 4884.
(16) Lemmens, P.; Choi, K.-Y.; Kaul, E. E.; Geibel, C.; Becker, K.; Brenig, W.; Valenti, R.; Gros, C.; Johnsson, M.; Millet, P.; Mila, F. *Phys. Rev. Lett*. **2001**, *87*, 227201.
(17) Moore, C. A.; Cussen, E. J.; Battle, P. D. *J. Solid State Chem*. **2000**, *153*, 254.
(18) Whangbo, M.-H.; Koo, H.-J. *Inorg. Chem*. **2002**, *41*, 3570.
(19) Dai, D.; Koo, H.-J.; Whangbo, M.-H. In *Solid State Chemistry of Inorganic Materials III*; Geselbracht, M. J., Greedan, J. E., Johnson, D. C., Subramanian, M. A., Eds.; MRS Symposium Proceedings, Vol. 658; Materials Research Society, Warrendale, PA, 2001; GG5.3.1−5.3.11.
(20) Whangbo, M.-H.; Koo, H.-J.; Dai, D.; Jung, D. *Inorg. Chem*. **2002**, *41*, 5575.
(21) Koo, H.-J.; Whangbo, M.-H.; Lee, K.-S. *J. Solid State Chem*. **2002**, *169*, 143.
(22) For a recent review, see: Whangbo, M.-H.; Koo, H.-J.; Dai, D. *J. Solid State Chem*., submitted for publication.
(23) Kahn, O. *Molecular Magnetism*: VCH Publishers: Weinheim, 1993.

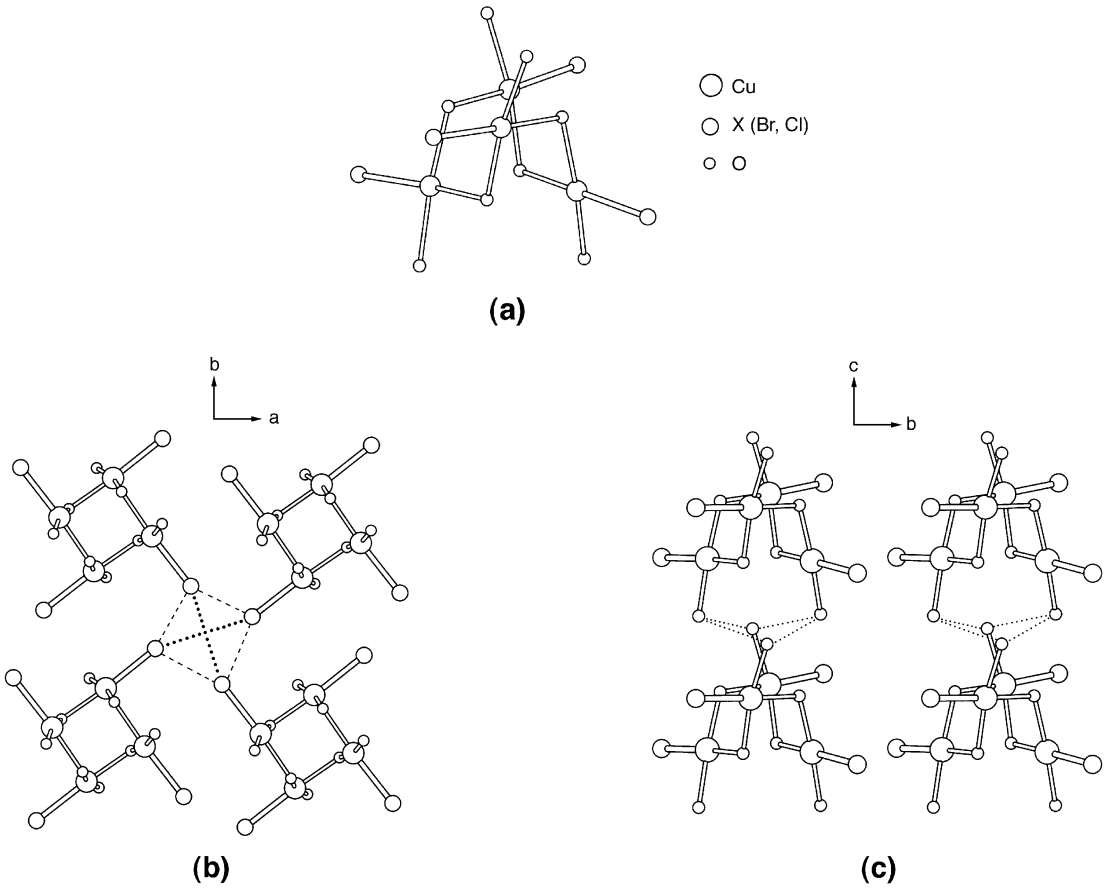

Figure 2. (a) $Cu_4O_8X_4$ cluster of $Cu_2Te_2O_5X_2$. (b) X···X contacts within a layer of $Cu_4O_8X_4$ clusters parallel to the *ab*-plane. (c) O···O contacts between neighboring layers of $Cu_4O_8X_4$ clusters.

as both ∠Cu−L···L bond angles become larger and as the L···L distance becomes shorter. Consequently, among SSE interactions with similar L···L distances, the stronger SSE interaction should have a longer Cu···Cu distance (Figure 1b,c).

The qualitative rule for SSE interactions enables us to predict whether a given SSE interaction would be strong or weak, once it is recognized what ranges of the L···L distance and the ∠Cu−L···L angles give rise to strong SSE interactions. The magnetic oxides $CuWO_4$ and $CuMoO_4$-III provide various SE and SSE interaction paths involving Cu^{2+} ions.[7,8] The spin dimer analysis [11] of these compounds showed that the strongest spin exchange interactions are given by the SSE interactions involving the most linear Cu−O···O−Cu paths. The O···O distances of these paths are in the range of 2.4 Å, which is considerably shorter than the van der Waals distance (i.e., 2.8 Å), and the two ∠Cu−O···O angles of these paths are identical and are close to 165°. As a rule of thumb, it is reasonable to suppose that the SSE interaction of a Cu−L···L−Cu path is strong when the L···L distance is close to or shorter than the van der Waals distance and when both ∠Cu−L···L bond angles are in the range of 160° and larger.

Obviously, the relative strengths of SE and SSE interactions of a magnetic solid cannot be determined unless appropriate electronic structure calculations are carried out. This topic will be discussed in section 4.

3. Superexchange and Super-Superexchange Paths

A. $Cu_2Te_2O_5X_2$. The compounds $Cu_2Te_2O_5X_2$ (X = Cl, Br)[13] consist of layers of tetrahedral clusters $Cu_4O_8X_4$. Each $Cu_4O_8X_4$ cluster is made up of four "square planar" CuO_3X units, which are joined by oxygen-corner-sharing such that the four Cu^{2+} ions form a tetrahedron and are linked by four SE paths Cu−O−Cu (Figure 2a). The $Cu_4O_8X_4$ clusters form layers parallel to the *ab*-plane (Figure 2b), in which the four Cu−X bonds of each cluster are pointed away from it toward the neighboring clusters so that every four adjacent $Cu_4O_8X_4$ clusters form a X_4 tetrahedron of short X···X contacts. Thus within a layer of $Cu_4O_8X_4$ clusters, there occur SSE interactions between adjacent clusters through the Cu−X···X−Cu paths. Between adjacent layers of $Cu_4O_8X_4$ clusters (Figure 2c), the clusters interact through short O···O contacts thus forming SSE interaction paths Cu−O···O−Cu. The geometrical parameters associated with the various SE and SSE paths of $Cu_2Te_2O_5X_2$ (X = Cl, Br) are summarized in Table 1a−c.

The magnetic susceptibility data of $Cu_2Te_2O_5X_2$ (X = Cl, Br) were interpreted by supposing[13−15] that the strongly interacting spin units of $Cu_2Te_2O_5X_2$ are $Cu_4O_8X_4$ clusters, and the interactions between clusters are weak. The topology of the spin exchange interactions in an isolated $Cu_4O_8X_4$ cluster is given by a tetrahedron of four spin sites as depicted in Figure 3, where the four exchange paths J_1 refer to the four SE paths Cu−O−Cu, and the two exchange paths

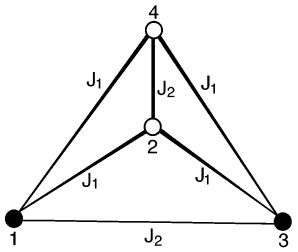

Figure 3. Strongly interacting spin unit based on an isolated $Cu_4O_8X_4$ cluster of $Cu_2Te_2O_5X_2$ proposed in refs 11−13, where the circles represent Cu^{2+} ions. The open circles lie above the filled circles along the *c*-direction.

Table 1. Geometrical Parameters (Lengths, Å; Angles, deg) Associated with the Intracluster SE Paths and the Intercluster SSE Paths in $Cu_2Te_2O_5X_2$ (X = Cl, Br)

(a) Intracluster SE Paths Cu−O−Cu

	X = Cl	X = Br
Cu−O	1.971, 1.976	1.964, 2.013
∠Cu−O−Cu	109.8	106.9
Cu···Cu	3.230	3.195

(b) Intercluster SSE Paths Cu−X···X−Cu

	X = Cl	X = Br
Along the ($a \pm b$)-Direction		
Cu···Cu	8.032	8.439
X···X	3.667	3.835
∠Cu−X···X	164.3, 164.3	154.4, 154.4
Along the *a*- and *b*-Directions		
Cu···Cu	6.020	6.289
X···X	3.516	3.588
∠Cu−X···X	125.3, 108.1	129.3, 105.5

(c) Intercluster SSE Path Cu−O···O−Cu

	X = Cl	X = Br
Cu···Cu	5.015	5.059
O···O	3.011	2.998
∠Cu−O···O	83.4, 105.4	85.6, 106.5

J_2 to the two SSE paths Cu−O···O−Cu. The fitting of the magnetic susceptibility data with the spin Hamiltonian,

$$\hat{H} = -J_1(\vec{S}_1\cdot\vec{S}_2 + \vec{S}_2\cdot\vec{S}_3 + \vec{S}_3\cdot\vec{S}_4 + \vec{S}_4\cdot\vec{S}_1) - J_2(\vec{S}_1\cdot\vec{S}_3 + \vec{S}_2\cdot\vec{S}_4)$$

revealed that $J_1 \approx J_2$ for both $Cu_2Te_2O_5Cl_2$ and $Cu_2Te_2O_5Br_2$. This result is quite surprising, as pointed out by Johnsson et al.[13] The magnetic orbital of a CuO_3X square planar unit is contained in the plane (Figure 1a) so that the two magnetic orbitals associated with a J_2 path should be nearly parallel to each other (Figure 2a) and hence their overlap should be practically zero. Therefore, the J_2 path should be very weakly antiferromagnetic, if not ferromagnetic. In addition, the ∠Cu−O−Cu angles of the SE paths Cu−O−Cu are much closer to 90° than to 180° (Table 1a), so that the antiferromagnetic interaction J_1 cannot be strong according to Goodenough rules.[12]

The Cu−X···X−Cu paths along the ($a \pm b$)-direction are the most linear SSE paths (Table 1b). In the most linear Cu−Cl···Cl−Cu path of $Cu_2Te_2O_5Cl_2$, the Cl···Cl distance (3.667 Å) is close to the van der Waals distance (i.e., 3.6 Å) while both ∠Cu−Cl···Cl bond angles are slightly larger than 160° (i.e., 164.3°). In the most linear Cu−Br···Br−Cu path of $Cu_2Te_2O_5Br_2$, the Br···Br distance (3.835 Å) is slightly shorter than the van der Waals distance (i.e., 3.9 Å) while both ∠Cu−Br···Br bond angles are slightly smaller than 160° (i.e., 154.4°). Consequently, the Cu−X···X−Cu paths along the ($a \pm b$)-direction can provide very strong antiferromagnetic interactions and hence should not be neglected.

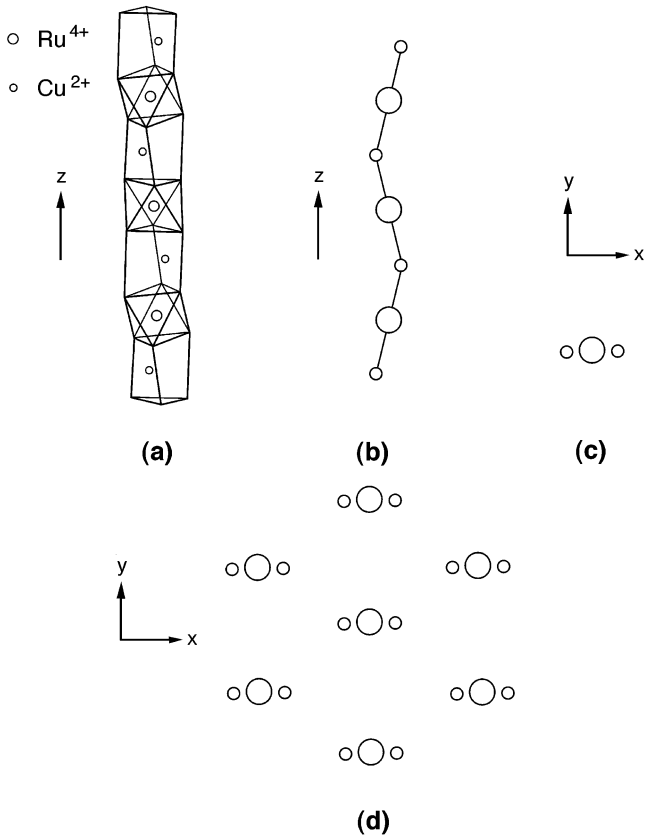

Figure 4. (a) Perspective polyhedral view of a $CuRuO_6$ chain in $Ca_{3.1}Cu_{0.9}RuO_6$. (b) Schematic perspective view of a CuRu zigzag chain. (c) Schematic projection view of a CuRu zigzag chain along the chain direction. (d) Schematic projection view of the CuRu zigzag chains in $Ca_{3.1}Cu_{0.9}RuO_6$ along the chain direction.

The spin monomers (i.e., structural units possessing one spin site) of $Cu_2Te_2O_5X_2$ (X = Cl, Br) are given by the distorted square planar units CuO_3X. Spin dimers with a SE path Cu−O−Cu are represented by $Cu_2O_5X_2$, and those with a SSE path Cu−L···L−Cu (L = X, O) by $Cu_2O_6X_2$.

B. $Ca_{3.1}Cu_{0.9}RuO_6$. This compound consists of $(Cu_{0.9}Ca_{0.1})$-RuO_6 chains separated by Ca^{2+} ions.[16] Figure 4a depicts an idealized $CuRuO_6$ chain, in which RuO_6 octahedra alternate with CuO_6 trigonal prisms by sharing their triangular faces. When the Cu positions of the trigonal prisms are statistically occupied by Cu and Ca in a 9:1 ratio, the $(Cu_{0.9}Ca_{0.1})RuO_6$ chains of $Ca_{3.1}Cu_{0.9}RuO_6$ result. For simplicity, we will discuss hereafter as if the trigonal prisms are all occupied by Cu atoms. In each CuO_6 trigonal prism the Cu atom is located on one of the three rectangular faces in such a way that the occupied rectangular faces in every pair of adjacent CuO_6 trigonal prisms of a $CuRuO_6$ chain are farthest apart from each other. Therefore, the Cu and Ru atoms of the $CuRuO_6$ chain form a "CuRu" zigzag chain (Figure 4b). The projection view of this zigzag chain along the chain direction can be represented as shown in Figure 4c. Then the

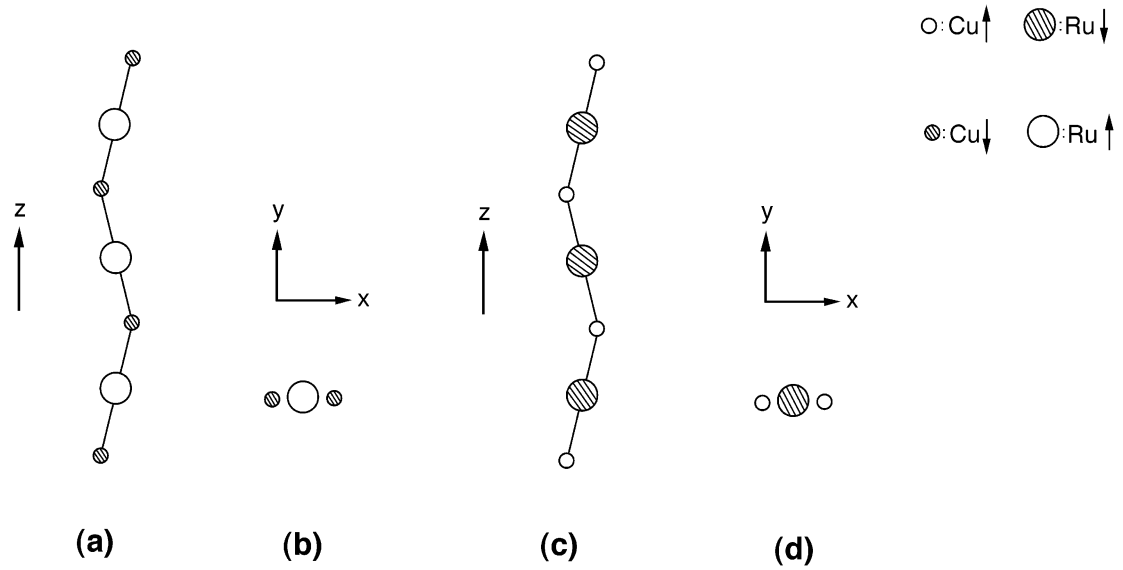

Figure 5. (a) Schematic perspective view of a ferrimagnetically ordered CuRu zigzag chain. (b) Schematic projection view of the ferrimagneic CuRu zigzag chain of Figure 5a along the chain direction. (c) Schematic perspective view of a ferrimagnetically ordered CuRu zigzag chain. (d) Schematic projection view of the ferrimagneic CuRu zigzag of Figure 5c along the chain direction.

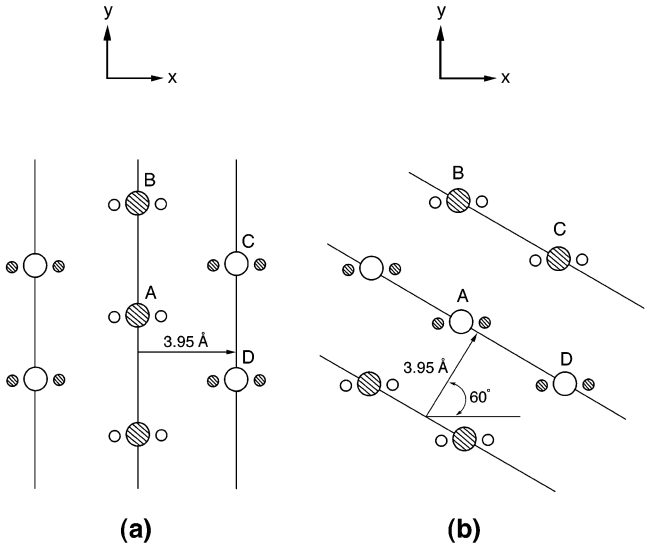

Figure 6. Interactions between the ferrimagnetic CuRu zigzag chains in $Ca_{3.1}Cu_{0.9}RuO_6$: (a) 3D arrangement proposed in ref 16; (b) 3D arrangement predicted from the present spin dimer analysis. Each solid line represents the plane containing ferromagnetically ordered CuRu zigzag chains.

arrangement of the $CuRuO_6$ chains in $Ca_{3.1}Cu_{0.9}RuO_6$ is represented as shown in Figure 4d.

The powder neutron diffraction measurements[16] of $Ca_{3.1}Cu_{0.9}RuO_6$ suggest collinear ferrimagnetic ordering of the Cu and Ru spins within each chain and antiferromagnetic interchain coupling. It is convenient to represent the ferrimagnetically ordered spin arrangement of a $CuRuO_6$ chain in Figure 5a by the projection view of Figure 5b, and that of a $CuRuO_6$ chain in Figure 5c by the projection view of Figure 5d. Then the three-dimensional (3D) arrangement of spins proposed by Moore et al.[16] can be represented as in Figure 6a, in which the chains are ferromagnetically coupled in each layer of chains parallel to the *yz*-plane, and these layers are antiferromagnetically coupled along the *x*-direction. This picture of interchain coupling is not consistent with the strongest interchain SSE interactions present in $Ca_{3.1}Cu_{0.9}RuO_6$. Analysis of the crystal structure of $Ca_{3.1}Cu_{0.9}RuO_6$ shows that the most linear Cu−O···O−Cu paths occur within each layer of chains parallel to the *yz*-plane (Figures 7a,b). The O···O distance (i.e., 2.849 Å) of these paths is close to the van der Waals distance (i.e., 2.8 Å), but both ∠Cu−O···O angles of these paths are somewhat smaller than 160° (i.e., 142.8°). Thus, the SSE interaction associated with this Cu−O···O−Cu path may not be very strong but can still be substantially antiferromagnetic. If so, the interchain interactions within each layer parallel to the *yz*-plane would be antiferromagnetic (Figures 6b and 7c) rather than ferromagnetic.

In $Ca_{3.1}Cu_{0.9}RuO_6$, the spin monomer for each Cu^{2+} site is given by the distorted square planar unit CuO_4, and that for each Ru^{4+} site by the distorted octahedron RuO_6, which has four magnetic orbitals. The spin dimer representing the SE interaction between adjacent Ru^{4+} and Cu^{2+} ions of a $CuRuO_6$ chain is given by $RuCuO_9$. The spin dimer representing the SSE interaction between two adjacent Ru^{4+} ions is Ru_2O_{12}, and that between two adjacent Cu^{2+} ions is Cu_2O_8.

4. Spin Dimer Analysis

The spin exchange parameters *J* can be determined from first-principles electronic structure calculations for the high- and low-spin states of spin dimers.[24−26] They can also be determined from first-principles electronic band structure calculations for various ordered spin arrangements of a magnetic solid.[27] These quantitative approaches become impractical for magnetic solids with large and complex unit cell structures. In explaining the anisotropy of spin exchange

(24) Illas, F.; Moreira, I. de P. R.; de Graaf, C.; Barone, V. *Theor. Chem. Acc.* **2000**, *104*, 265 and the references therein.
(25) Noodleman, L. *J. Chem. Phys.* **1981**, *74*, 5737.
(26) Dai, D.; Whangbo, M.-H. *J. Chem. Phys.* **2001**, *114*, 2887; **2003**, *118*, 29.
(27) Derenzo, S. E.; Klitenberg, M. K.; Weber, M. J. *J. Chem. Phys.* **2000**, *112*, 2074 and the references therein.

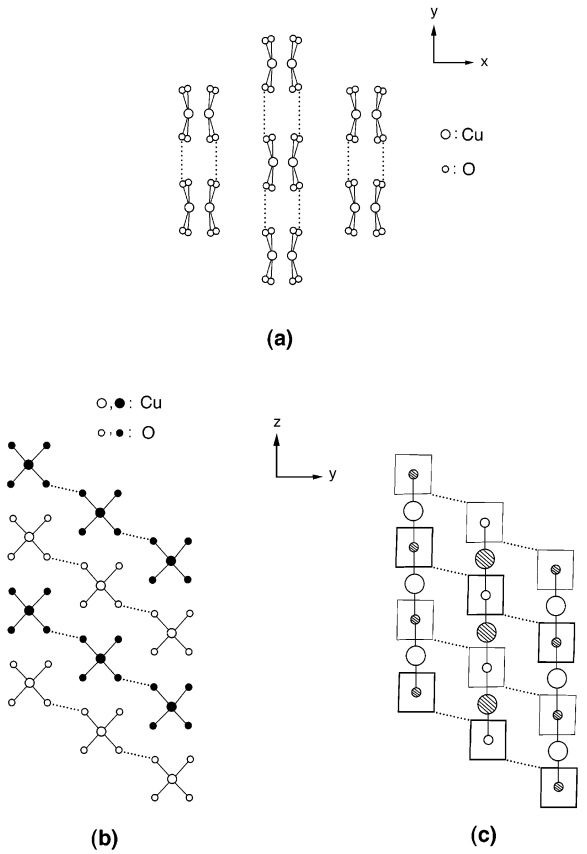

Figure 7. (a) Schematic projection view of the square planar CuO_4 units of the $CuRuO_6$ chains along the chain direction, where the dotted lines refer to the short O···O contacts that occur between adjacent $CuRuO_6$ chains. For simplicity, the Ru atoms are not shown. (b) Schematic projection view of square planar CuO_4 units of the $CuRuO_6$ chains (within a layer parallel to the *yz*-plane) along the *x*-direction. The and CuO_4 units with filled and open circles refer to those at different heights along the *x*-axis. (c) Antiferromagnetic arrangement between CuRu chains in a layer of $CuRuO_6$ chains parallel to the *yz*-plane, where each rectangle represents the O_4 rectangle of each CuO_4 square planar unit.

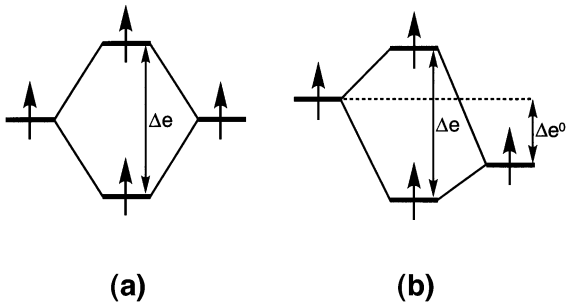

Figure 8. Spin orbital interaction energies associated with the interactions (a) between two equivalent magnetic orbitals and (b) between two nonequivalent magnetic orbitals.

interactions of magnetic solids, it is sufficient to estimate the relative magnitudes of their *J* values.[9−11,17−21]

Suppose that each spin site of a spin dimer contains one unpaired electron, and the two spin sites are equivalent (Figure 8a) and represented by nonorthogonal magnetic orbitals (i.e., singly occupied molecular orbitals) ϕ_1 and ϕ_2 of the spin monomers. Provided that *S* and Δe are respectively the overlap integral and the spin orbital interaction energy between ϕ_1 and ϕ_2, then the J_{AF} term varies as $J_{AF} \propto -(\Delta e)^2 \propto -S^2$. When the two spin sites of a spin dimer are nonequivalent (Figure 8b), the two magnetic orbitals differ in energy by Δe^0. For qualitative purposes, the extent of the antiferromagnetic spin exchange interaction can be discussed in terms of the net spin orbital interaction energy, $(\Delta e - \Delta e^0)$. For semiquantitative purposes, however, it is necessary to employ the spin orbital interaction $\Delta\epsilon = [(\Delta e)^2 - (\Delta e^0)^2]^{1/2}$.[10,22] The Δe^0 value can be estimated from the energies of the magnetic orbitals calculated for the spin monomers representing the two spin sites. Obviously, $\Delta e^0 = 0$, when the two spin sites are equivalent. For the simplicity of our notation, we will use the symbol $\Delta\epsilon$ to represent Δe for the case of two equivalent spin sites, and $[(\Delta e)^2 - (\Delta e^0)^2]^{1/2}$ for the case of two nonequivalent spin sites. The spin orbital interaction energy $\Delta\epsilon$ is approximately twice the hopping integral t (i.e., the resonance integral between ϕ_1 and ϕ_2), i.e., $\Delta\epsilon \approx 2t$. Thus the following relationship holds:[10,17,20−23,28,29]

$$J_{AF} = -4t^2/U_{eff} \approx -(\Delta\epsilon)^2/U_{eff}$$

where U_{eff} is the effective on-site repulsion. For a given magnetic solid, the U_{eff} value would be nearly constant so that the relative magnitudes of J_{AF} values can be estimated by comparing those of the corresponding $(\Delta\epsilon)^2$ values.

The above discussion is sufficient for describing the SE and SSE interactions involving only Cu^{2+} ions. For the spin exchange interactions of $Ca_{3.1}Cu_{0.9}RuO_6$, we need to consider spin exchange interactions between Ru^{4+} ions as well as those between Cu^{2+} and Ru^{4+} ions. When two adjacent spin sites have M and N unpaired spins, respectively, the trends in spin exchange parameters can be discussed in terms of the average spin orbital interaction energies defined by[18−21]

$$\langle(\Delta e)^2\rangle = \frac{1}{MN}\sum_{\mu=1}^{M}\sum_{\nu=1}^{N}(\Delta\epsilon_{\mu\nu})^2$$

The $Ru^{4+}(d^4)$ ion in each slightly distorted RuO_6 octahedron of $Ca_{3.1}Cu_{0.9}RuO_6$ has the local electron configuration $(t_{2g})^3(e_g)^1$. The three t_{2g}-block levels of each Ru^{4+} site may be labeled as ϕ_1, ϕ_2, and ϕ_3, and the two e_g-block levels of each Ru^{4+} site as ϕ_4 and ϕ_5. Likewise, the magnetic orbital of each distorted square planar CuO_4 unit may be represented by ϕ_0. Thus the configuration $(t_{2g})^3(e_g)^1$ of a $Ru^{4+}(d^4)$ ion can be represented either by $(\phi_1)^1(\phi_2)^1(\phi_3)^1(\phi_4)^1$ or by $(\phi_1)^1(\phi_2)^1(\phi_3)^1(\phi_5)^1$. If we assume that these two configurations are equally important, then the $(\Delta\epsilon_{\mu\nu})^2$ value for the SE interaction between adjacent Ru^{4+} and Cu^{2+} ions of a $CuRuO_6$ chain can be evaluated by the expression

$$\langle(\Delta\epsilon)^2\rangle = \frac{1}{4}\Big\{(\Delta\epsilon_{01})^2 + (\Delta\epsilon_{02})^2 + (\Delta\epsilon_{03})^2 + \frac{1}{2}[(\Delta\epsilon_{04})^2 + (\Delta\epsilon_{05})^2]\Big\}$$

Likewise, the $\langle(\Delta\epsilon)^2\rangle$ value for the SSE interactions between two adjacent Ru^{4+} ions can be written as

(28) Ginsberg, A. P. *Inorg. Chim. Acta, Rev.* **1971**, *5*, 45.
(29) This expression is valid when spin exchange parameters of a spin Hamiltonian are written as *J* instead of 2*J*.

$$\langle(\Delta\epsilon)^2\rangle = \frac{1}{16}\Big\{(\Delta\epsilon_{11})^2 + (\Delta\epsilon_{22})^2 + (\Delta\epsilon_{33})^2 + \frac{1}{4}[(\Delta\epsilon_{44})^2 + (\Delta\epsilon_{55})^2]\Big\}$$

by noting that $\Delta\epsilon_{\mu\nu}$ between equivalent spin sites is zero when the magnetic orbitals ϕ_μ and ϕ_ν are different in symmetry so that $S_{\mu\nu} = 0$, and is negligible when ϕ_μ and ϕ_ν are different in shape so that $S_{\mu\nu}$ is negligibly small.[18−21]

In describing the spin exchange interactions of magnetic solids in terms of $\Delta\epsilon$ values obtained from extended Hückel molecular orbital calculations,[30,31] it is necessary[9−11,17−21] to employ double-ζ Slater-type orbitals (STOs) [32] for both the d orbitals of the transition metal and the s/p orbitals of the surrounding ligand atoms. The atomic orbital parameters of Cu, Ru, O, Cl, and Br employed for our calculations are summarized in Table 2. The radial part of the *n*p orbital, $\chi_{np}(r)$, of the ligand atom L (=O, Cl, Br) is written as

$$\chi_{np}(r) = r^{n-1}[C\exp(-\zeta r) + C'\exp(-\zeta' r)]$$

where the exponents ζ and ζ' describe contracted and diffuse STOs, respectively (i.e., $\zeta > \zeta'$). The diffuse STO provides an orbital tail that enhances overlap between L atoms in the short L···L contacts of the SSE path M−L···L−M as well as that between the SE path M−L−M. The $\Delta\epsilon$ values are affected most sensitively by the exponent ζ' of the diffuse STO of the L *n*p orbital. Our studies[10,17,19−21] on other magnetic solids show that the ζ' value appropriate for studying spin exchange interactions of magnetic oxides should be increased from that obtained by Clementi and Roetti[32] from their atomic calculations by 10−13%. The ζ' values of the ligand *n*p orbitals listed in Table 2 are those increased by 12.5%.

The strength of a SE or SSE interaction is evaluated by using the Δe value from the spin dimer and the Δe_0 values calculated from the spin monomers. In evaluating the strength of a SSE interaction between two magnetic orbitals ϕ_μ and ϕ_ν, the Δe value can be evaluated by using their hopping integral $t_{\mu\nu} = \langle\phi_\mu|H^{\text{eff}}|\phi_\nu\rangle$ and overlap integral $S_{\mu\nu} = \langle\phi_\mu|\phi_\nu\rangle$, when the magnetic orbitals ϕ_μ and ϕ_ν interact not only between them but also with other orbitals in a given spin dimer. The $t_{\mu\nu}$ and $S_{\mu\nu}$ values are easily obtained by performing fragment molecular orbital analysis for a given spin dimer.[33]

5. Results and Discussion

A. $Cu_2Te_2O_5X_2$. The $(\Delta\epsilon)^2$ values calculated for the intra- and the intercluster spin exchange interactions (Figure 9) of $Cu_2Te_2O_5Cl_2$ and $Cu_2Te_2O_5Br_2$ are summarized in Table 3a,b. The $(\Delta\epsilon)^2$ values for the Cu−O···O−Cu paths between adjacent layers of clusters are not listed because they are negligibly small. This result is expected because the ∠Cu−O···O angles of the SSE paths Cu−O···O−Cu between adjacent layers of tetrahedral clusters (Figure 2c) are also much closer to 90° than to 180° (Table 1c). The intracluster SSE interaction J_2 of $Cu_2Te_2O_5X_2$ (X = Cl, Br) is also negligibly small for the same reason. The intracluster SE interaction J_1 is also weak as anticipated, because the ∠Cu−O−Cu angles of the SE paths Cu−O−Cu are close to 90° (Table 1a).

In $Cu_2Te_2O_5X_2$ (X = Cl, Br) the intercluster SSE interaction J_a is by far the strongest spin exchange interaction. As expected, this interaction involves the most linear Cu−X···X−Cu path, which occurs along the ($a \pm b$)-direction in each layer of tetrahedral clusters. The Cu−X···X−Cu paths along the *a*- and *b*-directions are significantly less linear than those along the ($a \pm b$)-direction (Table 1b) and hence lead to weaker antiferromagnetic interactions.

The $(\Delta\epsilon)^2$ values of Table 3 suggest that the magnetic properties of $Cu_2Te_2O_5Cl_2$ and $Cu_2Te_2O_5Br_2$ should be

Table 2. Exponents ζ_i and Valence Shell Ionization Potentials H_{ii} of Slater-Type Orbitals χ_i Used for Extended Hückel Tight-Binding Calculation[a]

atom	χ_i	H_{ii} (eV)	ζ_i[b]	C	ζ'_i[b]	C'
Cu	4s	−11.4	2.151	1.0		
Cu	4p	−6.06	1.370	1.0		
Cu	3d	−14.0	7.025	0.4473	3.004	0.6978
Ru	5s	−10.4	2.091	1.0		
Ru	5p	−6.87	1.420	1.0		
Ru	4d	−14.9	4.357	0.5394	2.265	0.6062
O	2s	−32.3	2.688	0.7076	1.675	0.3745
O	2p	−14.8	3.694	0.3322	1.866	0.7448
Cl	3s	−26.3	2.297	0.6262	1.854	0.5051
Cl	3p	−14.2	2.624	0.5554	1.659	0.5519
Br	4s	−22.1	3.361	0.6310	2.044	0.5050
Br	4p	−13.1	2.920	0.5822	1.827	0.5472

[a] H_{ii}'s are the diagonal matrix elements $\langle\chi_i|H^{\text{eff}}|\chi_i\rangle$, where H^{eff} is the effective Hamiltonian. In our calculations of the off-diagonal matrix elements $H_{ij} = \langle\chi_i|H^{\text{eff}}|\chi_j\rangle$, the weighted formula was used. See: Ammeter, J.; Bürgi, H.-B.; Thibeault, J.; Hoffmann, R. *J. Am. Chem. Soc*. 1978, *100*, 3686. [b] Contraction coefficients used in the double-ζ Slater-type orbital.

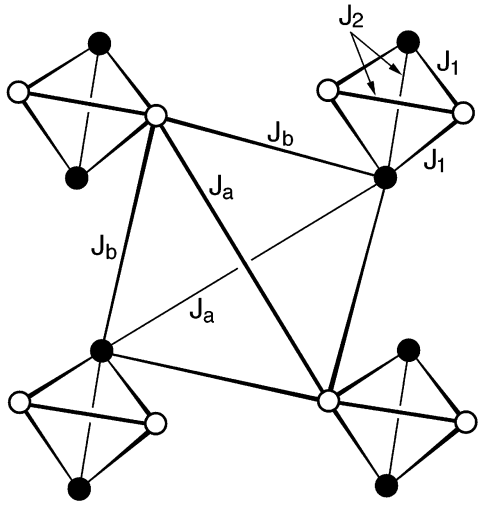

Figure 9. Spin exchange paths in a layer of $Cu_4O_8X_4$ clusters in $Cu_2Te_2O_5X_2$, where the circles represent Cu^{2+} ions. The unshaded circles lie above the shaded circles along the *c*-direction. J_1 and J_2 are intracluster spin exchange interactions, and J_a and J_b are intercluster spin exchange interactions.

(30) Hoffmann, R. *J. Chem. Phys*. **1963**, *39*, 1397.
(31) Our calculations were carried out by employing the CAESAR2 and SAMOA program packages (Dai, D.; Ren, J.; Liang, W.; Whangbo, M.-H. http://primec.ncsu.edu/, 2002).
(32) Clementi, E.; Roetti, C. *At. Data Nucl. Data Tables* **1974**, *14*, 177.
(33) Albright, T. A.; Burdett, J. K.; Whangbo, M.-H. *Orbital Interactions in Chemistry*: Wiley: New York, 1985.

Table 3. $(\Delta\epsilon)^2$ Values in Units of $(meV)^2$ Calculated for the Various SE and SSE Interactions of $Cu_2Te_2O_5X_2$

interaction	path	Cu···Cu (Å)	$(\Delta\epsilon)^2$	rel strength
		(a) $Cu_2Te_2O_5Cl_2$		
SE	J_1	3.230	576	0.10
	J_2	3.591	25	0.00
SSE	J_b	6.020	484	0.08
	J_a	8.032	5746	1.00
		(b) $Cu_2Te_2O_5Br_2$		
SE	J_1	3.195	676	0.01
	J_2	3.543	100	0.00
SSE	J_b	6.289	12410	0.19
	J_a	8.439	63958	1.00

slightly different. The relative magnitudes of the J_a, J_b, J_1, and J_2 interactions are given as follows:

$$J_a > J_1 \geq J_b > J_2 \qquad \text{for } Cu_2Te_2O_5Cl_2$$

$$J_a > J_b \gg J_1 > J_2 \qquad \text{for } Cu_2Te_2O_5Br_2$$

Thus both $Cu_2Te_2O_5Cl_2$ and $Cu_2Te_2O_5Br_2$ are described by weakly interacting dimers. The weak interdimer interactions lead to isolated tetrameric units (defined by J_a and J_b) in $Cu_2Te_2O_5Br_2$ and to a two-dimensional lattice (defined by J_a, J_1, and J_b) in $Cu_2Te_2O_5Cl_2$. It is important to note that the intracluster SE interaction is much stronger in $Cu_2Te_2O_5Cl_2$ than in $Cu_2Te_2O_5Br_2$. This reflects the fact that the Cu−O−Cu bridge is much more symmetrical in $Cu_2Te_2O_5Cl_2$ than in $Cu_2Te_2O_5Br_2$ (Table 1a). The recent study[19] of the SE interactions of $CaMn_2O_4$ showed that the SE interaction of an Mn−O−Mn path increases as the Mn−O−Mn bridge becomes more symmetrical and as the Mn−O bond length becomes shorter.

It is important to examine the validity of a weakly interacting dimer model for $Cu_2Te_2O_5X_2$ (X = Cl, Br) from the viewpoint of simulating the experimental susceptibility curve $\chi_{exp}(T)$ of $Cu_2Te_2O_5X_2$ reported by Johnsson et al.[13] For this purpose, we fitted the χ_{exp} data with the calculated susceptibility curve χ_{calc} with a Weiss correction, i.e.,

$$\chi_{exp} = \chi_{calc}/(1 - \theta\chi_{calc})$$

where $\theta = 2zJ'/(Ng^2\beta^2)$.[34] The calculated susceptibility χ_{calc} is written as

$$\chi_{calc} = \chi_{vv} + \chi_{TIP} + C/T$$

where χ_{vv} is the Van Vleck term that depends on the spin exchange parameters, χ_{TIP} refers to the temperature-independent paramagnetism, and C/T is the term for the paramagnetic impurity. Our fitting analysis of the experimental χ_{exp} data of Johnsson et al.[13] was carried out as described below.

(a) According to Table 3a and Figure 9, the spin exchange interactions of $Cu_2Te_2O_5Cl_2$ can be approximated by a tetramer model with the two intercluster interactions J_a and J_b in which the J_b/J_a ratio is approximately 0.1, if the intracluster interaction J_1 is neglected. Our analysis using this tetramer model led to the results $g = 2.01$, $J_a/k_B = -41.3$ K, $J_b/k_B = -5.1$ K, $zJ'/k_B = -0.0049$ K, $\chi_{TIP} = 0.000489$ emu/mol, $C = 0.0609$ emu·K/mol with the standard deviation 7.35×10^{-4}. The J_b/J_a ratio obtained from the fitting (i.e., 0.12) is in good agreement with the theoretical estimate from the spin dimer analysis.

(b) According to Table 3a and Figure 9, the spin exchange interactions of $Cu_2Te_2O_5Cl_2$ can also be regarded as an alternating Heisenberg chain with the intercluster interaction J_a and the intracluster interaction J_1 in which the J_1/J_a ratio is approximately 0.1, if the intercluster interaction J_b is neglected. In our fitting analysis for this model, we approximated the alternating chain with a linear hexamer in which the spin exchange paths are connected as $J_a-J_1-J_a-J_1-J_a$. Our fitting analysis with this hexamer model led to the results $g = 1.96$, $J_a/k_B = -47.4$ K, $J_1/k_B = -6.5$ K, $zJ'/k_B = -0.0055$ K, $\chi_{TIP} = 0.000588$ emu/mol, $C = 0.0664$ emu·K/mol with the standard deviation 8.90×10^{-4}. This hexamer model based on the inter- and intracluster interactions also gives an excellent fitting, and the J_1/J_a value thus obtained (i.e., 0.14) agrees well with the theoretical estimate based on the spin dimer analysis.

(c) According to Table 3b and Figure 9, the spin exchange interactions of $Cu_2Te_2O_5Br_2$ can be approximated by a tetramer model with the two intercluster interactions J_a and J_b in which the J_b/J_a ratio is approximately 0.2. Our fitting analysis using this tetramer model led to the results $g = 2.02$, $J_a/k_B = -49.8$ K, $J_b/k_B = -9.1$ K, $zJ'/k_B = -0.0050$ K, $\chi_{TIP} = 0.000874$ emu/mol, $C = 0.0191$ emu·K/mol with the standard deviation 5.88×10^{-3}. The J_b/J_a ratio thus obtained (i.e., 0.18) is in good agreement with the theoretical estimate from the spin dimer analysis.

As described above, for both $Cu_2Te_2O_5Cl_2$ and $Cu_2Te_2O_5Br_2$, the experimental χ_{exp} data of Johnsson et al.[13] are very well reproduced by using the models in which the relative strengths of the spin exchange parameters are determined by the spin dimer analysis. The key to the success of these simulations is that the strongest antiferromagnetic spin exchange interaction is given by the intercluster spin exchange J_a. Although the tetramer model based solely on the intracluster interactions (Figure 3) provides a good fitting, the two assumptions employed in this model (i.e., the neglect of the strong intercluster interaction J_a and the constraint $J_1 = J_2$) are inconsistent with electronic structure considerations as discussed above.

B. $Ca_{3.1}Cu_{0.9}RuO_6$. The $(\Delta\epsilon)^2$ values calculated for the intra- and the interchain spin exchange interactions of $Ca_{3.1}Cu_{0.9}RuO_6$ are summarized in Table 4. The strongest antiferromagnetic interactions are the SE interactions between the adjacent Cu^{2+} and Ru^{4+} ions in each $CuRuO_6$ chain, which lead to a ferrimagnetic ordering in each $CuRuO_6$ chain. This picture agrees with the assignment given by Moore et al.[16]

The second strongest antiferromagnetic interactions are the SSE interactions involving the most linear Cu−O···O−Cu paths, which are found between adjacent chains in each layer of $CuRuO_6$ chain parallel to the *yz*-plane (Figure 7a,b). All other intra- and interchain SSE paths give rise to very weak antiferromagnetic interactions and hence can be ferromag-

(34) O'Connor, C. J. *Prog. Inorg. Chem.* **1982**, *29*, 203.

Table 4. $(\Delta\epsilon)^2$ Values in Units of $(meV)^2$ Calculated for the Various SE and SSE Interactions of $Ca_{3.1}Cu_{0.9}RuO_6$

M···M (Å)	interaction	$(\Delta\epsilon)^2$	rel strength
	Intrachain		
2.787 (Cu···Ru)	SE	1296	1.00
5.467 (Ru···Ru)	SSE	36	0.03
5.574 (Cu···Cu)	SSE	64	0.05
	Interchain (between A and B)[a]		
6.474 (Cu···Cu)	SSE	196	0.15
5.720 (Cu···Cu)	SSE	4	0.00
5.617 (Ru···Ru)	SSE	16	0.01
6.474 (Ru···Ru)	SSE	1	0.00
	Interchain (between A and C)[a]		
4.799 (Cu···Cu)	SSE	4	0.00
6.455 (Cu···Cu)	SSE	0	0.00
5.649 (Ru···Ru)	SSE	9	0.01
6.455 (Ru···Ru)	SSE	4	0.00

[a] The chains A, B, and C are defined in Figure 7.

netic. Therefore, as suggested by the qualitative rule for SSE interactions, our spin dimer analysis shows that the interchain interactions should be antiferromagnetic within a layer parallel to the *yz*-plane (Figures 6b and 7c), but either weakly antiferromagnetic or ferromagnetic between layers parallel to the *yz*-plane. This result does not support the assignment of the interchain interaction (Figure 6a) proposed by Moore et al.[16] We now examine the validity of the 3D spin arrangement of Figure 6b from the viewpoint of simulating the 3.7 K powder neutron diffraction profile of Moore et al.[16] In the 3D spin arrangement of Figure 6b, layers of the ferromagnetically arranged chains repeat along the direction 60° away from the *x*-direction. In the 3D spin arrangement of Figure 6a, layers of the ferromagnetically arranged chains repeat along the *x*-direction. The layers of ferromagnetically arranged chains are separated practically by the same spacing (i.e., 3.95 Å) in the two 3D spin arrangements, so that both spin arrangements should be equally good in fitting the 3.7 K powder neutron diffraction profile of Moore et al.[16] The possibility of the 3D spin arrangement of Figure 6b was not considered in the fitting analysis of Moore et al.[16]

6. Concluding Remarks

The consideration of the p-orbital tails of the magnetic orbital of a Cu^{2+} ion leads to the qualitative rule for SSE interactions between Cu^{2+} ions: *the strength of the SSE interaction involving a path Cu−L···L−Cu should increase as both ∠Cu−L···L bond angles become larger and as the L···L distance becomes shorter*. Our spin dimer analysis of the strong Cu−O···O−Cu and Cu−X···X−Cu (X = Cl, Br) interactions indicates that, as a rule of thumb, the SSE interaction associated with a Cu−L···L−Cu path should be considered strong when the L···L distance is within the van der Waals distance and when both ∠Cu−L···L bond angles are in the range of 160° and larger. This qualitative rule will be useful in making sure that strong SSE interactions essential for the spin lattice of a magnetic solid containing Cu^{2+} ions are not neglected. Strongly interacting spin exchange paths are determined by the overlap between magnetic orbitals. For a magnetic solid of any interest, the magnetic orbital(s) are not atomic s orbitals so that the overlap between adjacent magnetic orbitals in a magnetic solid cannot be isotropic. Consequently, the strongly interacting spin unit of a magnetic solid does not necessarily have the same geometrical feature as the arrangement of its magnetic ions. It is important to assess the strongly interacting spin exchange paths of magnetic solids on the basis of appropriate electronic structure considerations.

Our spin dimer analysis for $Cu_2Te_2O_5X_2$ (X = Cl, Br) shows that the intercluster SSE interactions along the ($a \pm b$)-direction involving the most linear Cu−X···X−Cu (X = Cl, Br) paths are the strongest spin exchange interactions, as predicted by the qualitative rule. Weaker interactions occur between these dimers to form isolated tetrameric units in $Cu_2Te_2O_5Br_2$ and a two-dimensional lattice in $Cu_2Te_2O_5Cl_2$. Our spin dimer analysis for $Ca_{3.1}Cu_{0.9}RuO_6$ shows that the interactions between $CuRuO_6$ chains should be antiferromagnetic within each layer perpendicular to the plane of the CuRu zigzag chain, as expected by the qualitative rule, due to the SSE interactions involving the most linear Cu−O···O−Cu paths. The spin lattices of $Cu_2Te_2O_5X_2$ and $Ca_{3.1}Cu_{0.9}RuO_6$ deduced from our spin dimer analysis are consistent with the available magnetic data.

Acknowledgment. The work at North Carolina State University was supported by the Office of Basic Energy Sciences, Division of Materials Sciences, U.S. Department of Energy, under Grant DE-FG02-86ER45259. D.J. thanks Korea Research Foundation for the financial support under Grant 2000-015-DP0300. M.-H.W. wishes to thank the anonymous reviewers for their critical comments and Dr. P. Millet, Professor C. J. O'Conner, and Dr. C. C. Torardi for invaluable discussions.

IC020551L